Microscopic degradation mechanism of polyimide film caused by surface discharge under bipolar continuous square impulse voltage*

Luo Yang(罗 杨), Wu Guang-Ning(吴广宁)†, Liu Ji-Wu(刘继午), Peng Jia(彭 佳), Gao Guo-Qiang(高国强), Zhu Guang-Ya(朱光亚), Wang Peng(王 鹏), and Cao Kai-Jiang(曹开江)

School of Electrical Engineering, Southwest Jiaotong University, Chengdu 610031, *China*

(Received 2 May 2013; revised manuscript received 16 July 2013; published online 20 December 2013)

Polyimide (PI) film is an important type of insulating material used in inverter-fed motors. Partial discharge (PD) under a sequence of high-frequency square impulses is one of the key factors that lead to premature failures in insulation systems of inverter-fed motors. In order to explore the damage mechanism of PI film caused by discharge, an aging system of surface discharge under bipolar continuous square impulse voltage (BCSIV) is designed based on the ASTM 2275 01 standard and the electrical aging tests of PI film samples are performed above the partial discharge inception voltage (PDIV). The chemical bonds of PI polymer chains are analyzed through Fourier transform infrared spectroscopy (FTIR) and the dielectric properties of unaged and aged PI samples are investigated by LCR testers HIOKI 3532-50. Finally, the micro-morphology and micro-structure changes of PI film samples are observed through scanning electron microscopy (SEM). The results show that the physical and chemical effects of discharge cut off the chemical bonds of PI polymer chains. The fractures of ether bond (C–O–C) and imide ring (C–N–C) on the backbone of a PI polymer chain leads to the decrease of molecular weight, which results in the degradation of PI polymers and the generation of new chemical groups and materials, like carboxylic acid, ketone, aldehydes, etc. The variation of microscopic structure of PI polymers can change the orientation ability of polarizable units when the samples are under an AC electric field, which would cause the dielectric constant ε to increase and dielectric loss tan δ to decrease. The SEM images show that the degradation path of PI film is initiated from the surface and then gradually extends to the interior with continuous aging. The injection charge could result in the PI macromolecular chain degradation and increase the trap density in the PI polymer bulk.

Keywords: surface discharge, polyimide film, micro-morphology and micro-structure, degradation process

PACS: 77.55.–g, 52.80.Wq, 68.55.–a **DOI:** 10.1088/1674-1056/23/2/027703

1. Introduction

In recent years, many adjustable speed motors equipped with power electronic devices have been used in the electrical industry. Inverter-fed traction motors, as the typical drive equipment, are more and more widely used in high speed railways, of which the insulation systems are exposed to transient surge voltage stresses with steep fronts induced by the switching of insulated gate bipolar transistors (IGBT)[1,2] as shown in Fig. 1. Thus the electrical stress is different from those in the common sinusoidal (50 Hz or 60 Hz) conditions. The presence of partial discharge (PD) is a source of extremely harmful degradation of organic insulating materials, which would result in premature failure of the insulation system and shorter life expectancy of inverter-fed traction motors.[3–8] The aging processes and failure mechanisms under this special stress have been investigated in numerous studies. As is now well known, the supply voltage waveforms, generated by the converters, play a major role in insulation damage. However, the microscopic degradation mechanism of the insulating material is ambiguous.

Polyimide (PI) film, as a special type of engineering plastic film, is characterized by high temperature resistance (400 °C), low temperature tolerance (−269 °C), radiation resistance, and excellent dielectric property. It is widely used in turn-to-turn insulation and turn-to-ground insulation of inverter-fed motors as a kind of basic insulating material. However, the material will be aged gradually and eventually cannot implement its insulating function to the required standard over a period of aging time, and both its chemical composition and physical morphology may be changed.[9,10] The properties and structures of aged materials can be known through the modern material analysis method, such as scanning electron microscopy (SEM), Fourier transform infrared spectroscopy (FTIR), thermogravimetry (TG), etc. Currently, in many professional papers the erosion effects of insulating materials caused by surface discharge are discussed, and the research objects mainly include epoxy and its composites,[11–13] silicon rubber and its composites,[14,15]

*Project supported by the National Natural Science Foundation of China (Grant Nos. U1234202, U1134205, 51177136, and 51107104).

†Corresponding author. E-mail: gnwu@swjtu.cn

© 2014 Chinese Physical Society and IOP Publishing Ltd

polypropylene and its composites,[16,17] polyamide and its composites [18,19] and oil-impregnated insulation paper.[20,21] Therefore, there is also a great need for a better understanding of the microscopic aging mechanism of PI film material.

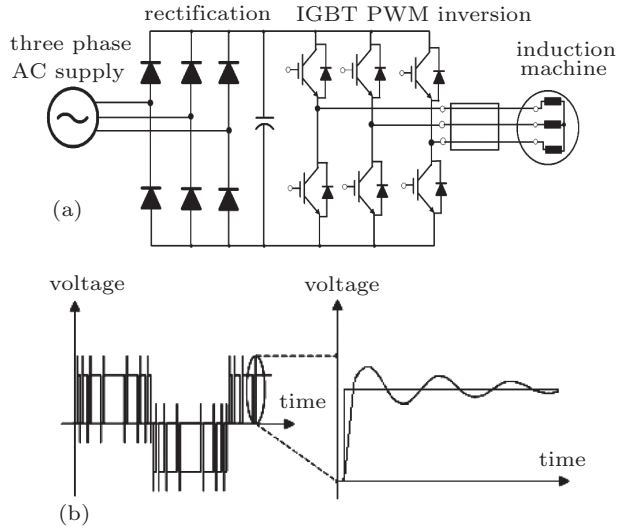


Fig. 1. (a) Schematic diagram of an inverter and (b) its output waveform.

In this paper, we focus on the microscopic damage mechanism of PI film samples which are stressed by electrical stresses of the bipolar continuous square impulse voltage (BCSIV) in the presence of discharge. Firstly, the molecular bonds of unaged and aged PI samples are revealed through the FTIR. Then the dielectric parameters of unaged and aged samples are measured and discussed, which indicate sufficiently the dipolar orientation polarization. Finally, the microscopic structural and morphological change processes of the PI samples are investigated by using SEM. Space charge distributions in PI samples are measured by using the pulsed electro-acoustic (PEA) method.

2. Experimental set-up

2.1. Aging condition

According to the criterion of IEC 60034-18-42, bipolar continuous square impulse voltage (BCSIV) could take the place of pulse width modulated (PWM) voltage for testing. The typical waveform of BCSIV can be seen in Fig. 2. The parameters of BCSIV, such as amplitude, repetition frequency and rising timel, can be adjusted conveniently. The partial discharge inception voltage (PDIV) for the PI samples is around 0.8 kV. The aging voltage of BCSIV is set to be 1 kV with a frequency of 1 kHz. The duty cycle is 0.5, rising time is 1 μs. The electrodes are designed based on the standard of ASTM-2275. The upper electrode is a cylinder with a diameter of 6 mm, the edge radius is 1 mm. The lower electrode is a plate electrode with a diameter of 51 mm. The materials of both electrodes are stainless steel.

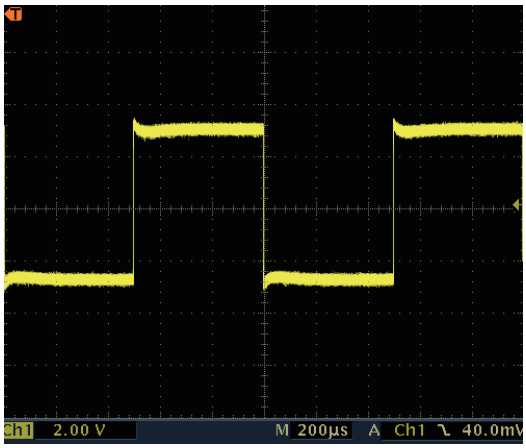


Fig. 2. (color online) Typical waveform used in test.

2.2. Samples

The PI film samples of 100HN are supplied by DUPONT Co., Ltd. The sizes of the samples are 50 mm×50 mm and 25-μm thick. All the samples are cleaned in absolute alcohol with 99.99% purity and dried in a heat oven at temperature of 60 °C for 2 h. Each specimen is placed between the upper and lower electrodes, which are connected to the high voltage terminal and low voltage terminal of BCSIV power respectively.

2.3. FTIR analysis

FTIR can be used to detect and identify the various polar chemical bonds. In this paper, the chemical bonds of aged and unaged PI samples are analyzed through FTIR. The wavenumber is in a range of 4000 cm^{-1}–700 cm^{-1}.

2.4. Dielectric analysis

In this paper, the values of the dielectric constant ε and dielectric loss tan δ of the polyimide film samples with different aging conditions are measured by using the LCR tester HIOKI 3532-50 and the frequency range is selected from 100 Hz to 1 MHz.

2.5. SEM analysis

The surface and sectional micrographs of samples in different aging states are investigated through scanning electron microscopy (SEM). When the high voltage is applied to the rod electrode, erosion caused by surface discharge happens around the upper electrode, whereas the area below the upper electrode is free of erosion as shown in Fig. 3(b).

As a low temperature resistance material, PI film is not brittle even in liquid helium below the temperature −269 °C. Thus it is difficult to obtain a good cross section of PI film. In this paper, the PI film samples are torn quickly after being cooled under liquid nitrogen for 1 h, in order to reduce

the damage to the cross section pattern. The section sketch is shown in Fig. 3(c).

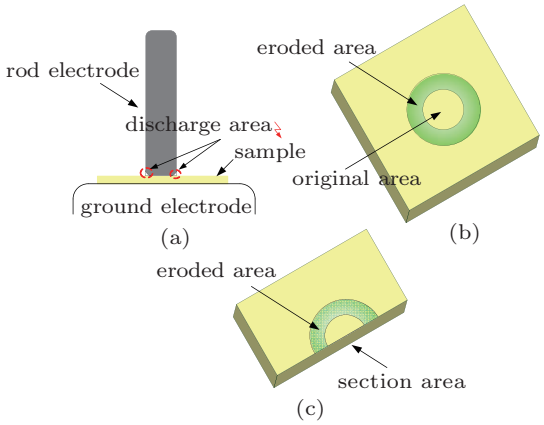


Fig. 3. (color online) Electrode configuration and eroded area of sample.

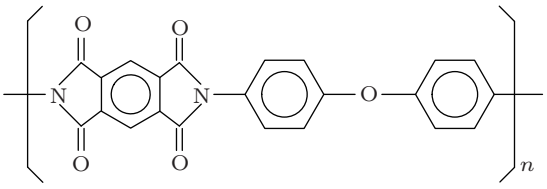
2.6. Space charge distribution

Space charge plays an important role in the aging process of polymer dielectrics. The threshold field of PI film for space charge accumulation is 31.5 kV/mm.[22] The aging field of PI film is 40 kV/mm, which is higher than the threshold field. Therefore, space charge will be injected into the PI film bulk and the space charge distribution is investigated by using the PEA method.[23] Polyimide films of 500HN are used to study the space charge accumulation because of the limit of measurement accuracy of the PEA method. The aging electrical field across a 500HN PI film is 40 kV/mm, which is equal to that across a 100HN film.

3. Results

3.1. Results of FTIR analysis

The degradation process of a polymer is the fracture of the molecule chain.[24,25] The molecule structure of a repeated unit of PI is sketched below.



The PI macromolecule compounded by the repeat units is a linear molecule chain consisting of heterocyclic rings (imide rings and aromatic rings) linked together with covalent bonds. Oxygen ether (C–O–C) with an angle of 126° results in the zigzag conformation of chain. The PI polymer chains are randomly arranged and wound with each other, which can provide the degree of cross linking for the PI polymer.

When a beam of infrared light with continuous frequency irradiates the sample, the infrared light according to a special chemical bond will be absorbed. The phenomena can be revealed from the spectrum. Therefore, FTIR can detect the types of chemical bonds and identify the type of material. In this paper, FTIR is used to analyze the changes of chemical bonds for the unaged and aged PI samples. The results for the unaged PI sample and aged samples with aging time from 1 h to 5 h are shown in Fig. 4. The reflectance peaks of unaged PI film at 1376 cm^{-1}, 1112 cm^{-1}, and 723 cm^{-1} relate to the bond of a C–N–C in imide ring, the 1776 cm^{-1} and 1716 cm^{-1} peaks are due to the vibration of C=O in imide ring. The reflectance peaks at 1240 cm^{-1} and 1456 cm^{-1} correspond to the bond of ether linkage (C–O–C). The other reflectance peaks, such as 1012 cm^{-1}, 1598 cm^{-1}, 1500 cm^{-1}, 1168 cm^{-1}, 1087 cm^{-1}, 883 cm^{-1}, etc., relate to the benzene ring.

Figure 4 shows the significant changes of FTIR spectra for aged PI samples compared with that for the unaged PI sample. When the PI film was aged for 1 h, the intensities of the reflectance peaks reduce because the structures and morphologies of chemical bonds have changed due to discharge erosion. The degree of cross linking of PI polymers decreases. The orientation ability of the dipolar group increases. When the PI film is aged for 3 h, the initiation of the fracture of molecule chain occurs. It is notable that the peaks of 1240 cm^{-1} and 1112 cm^{-1} disappear. It is suggested that the ether linkage (C–O–C) is broken and a ring-opening reaction occurs in the imide ring (C–N–C), which leads to the decrease of PI polymer molecular weight. A polyamic acid structure may be generated when the bonds of the imide ring (C–N–C) structure are broken.[26] The new reflectance peak of 1259 cm^{-1} corresponds to a C–O bond that may be derived from the fracture of ether linkage (C–O–C). The new peak of 2962 cm^{-1} could be assigned to the C-H stretching vibration of the methyl ($–CH_3$) or methylene group (–CH2–). The remaining two reflectance peaks at 1014 cm^{-1} and 798 cm^{-1} are attributed to the vibrations of aromatic rings. Moreover, at this point in time, the intensity of original reflectance peaks reduces more seriously. It is demonstrative that the chemical structure of PI molecules is affected. Some chemical bonds are broken down while some new chemical bonds are generated. After samples are aged for 5 h, more chemical bonds in aromatic rings and imide rings are broken, and the intensities of new peaks are enhanced. One more new peak appears at 1412 cm^{-1}, which may be assigned to the interaction of O–H deformation and C–O stretching vibrations. The vibrations of other original chemical bonds of PI molecules are very weak. It shows that the new chemical bonds are increased by the discharge and the structure of polyimide is destroyed almost entirely at this aging time.

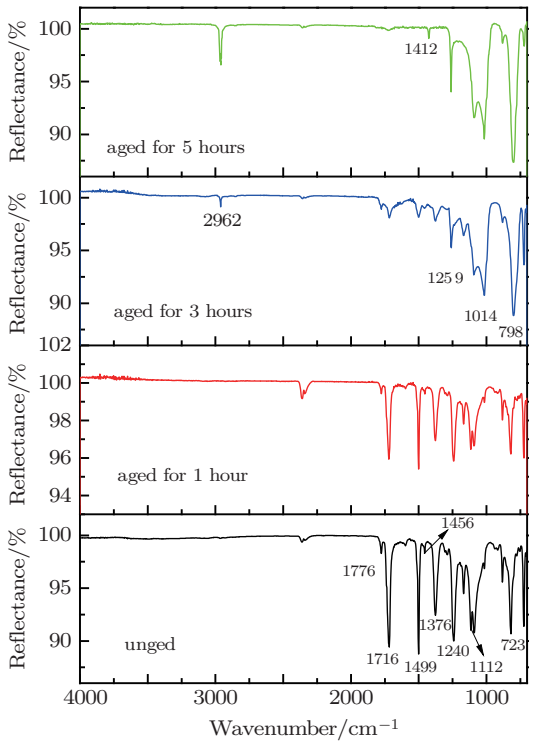


Fig. 4. (color online) FTIR spectra of unaged and aged PI films.

3.2. Results of dielectric analysis

The dielectric constant is dependent on the ability of the polarizable units under an alternating electric field, and dielectric loss tan δ is attributed to the friction interaction of polarizable units when the polarizable units orient at a certain frequency. When the polyimide samples are aged under an applied voltage, the chemical groups and the polarizable units are changed. It can influence the orientation polarization of dipolar groups.

Figure 5 shows the variations of the dielectric constant ε with frequency. For unaged and aged polyimide samples, each curve of the dielectric constant ε decreases with the increase of frequency. All the dielectric constants for aged samples are larger than those for unaged samples. The longer the aging time applied to the sample, the larger the dielectric constant value is, except for the sample aged for 6 h. The dielectric constant ε of the sample aged for 1 h increases more obviously. The polarizable units of PI samples have enough ability to follow the polarity variation of the applied electric field when the frequency varies from 100 Hz to 10^5 Hz. With the increase of frequency, polarizable units have not enough ability to orient following the applied electric field. Therefore, the dielectric constant ε remains nearly unchanged when the frequency ranges from 100 Hz to 10^5 Hz, and then ε decreases gradually when the frequency is in a range from 10^5 Hz to 10^6 Hz.

For unaged and aged polyimide samples, figure 6 shows the variations of the dielectric loss tan δ with frequency. The values of dielectric loss tan δ of all the samples increase with the increase of frequency. The values of dielectric loss tan δ of all the aged samples decrease clearly compared with that of the unaged sample. The longer the aging time applied to the sample, the smaller the dielectric loss, except for the sample aged for 6 h. At low frequencies, the cycle time of the applied alternating field is long enough that dipolar groups can follow the alternation of the applied field, resulting in low dielectric loss. When the frequency is in a higher frequency range, polarizable units do not have enough time to orient when the polarity of the applied electric field is alternated. The friction interaction among polarizable units will waste more energy which is supplied by the applied electric field, so the dielectric loss tan δ increases.

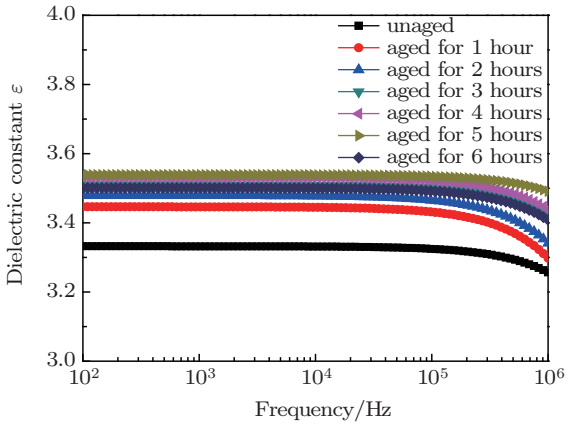


Fig. 5. (color online) Relationships between dielectric constant ε and frequency for unaged and aged polyimide samples.

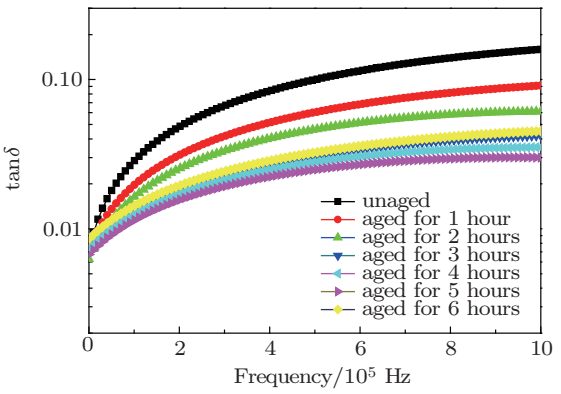
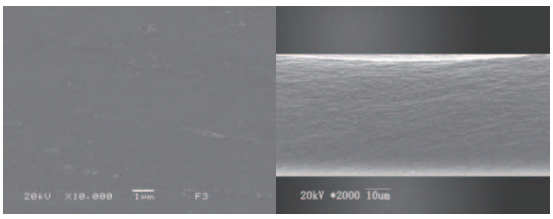


Fig. 6. (color online) Relationships between dielectric loss tan δ and frequency for unaged and aged polyimide samples.

3.3. Micro-morphology of unaged PI film

Figure 7 shows the surface and sectional micrographs of 100HN film. The surface of the unaged sample (Fig. 7(a)) is smooth and most parts of the sample are uniform with no layers (Fig. 7(b)).



(a) (b)

Fig. 7. Micrographs of (a) surface and (b) cross section of original 100HN sample.

3.4. Micro-morphology of aged PI film

Before the PI film is broken down, the damage to PI film concentrates on the surface of the sample when discharge occurs. Figure 8 shows the full view of the aging part. The area, which is under the top rod electrode, remains the original smooth morphology. The discharge appears around the edge of upper rod electrode. The surface of PI film in area is eroded as the consequence of surface discharge, which leads to the surface roughness and morphology changing.

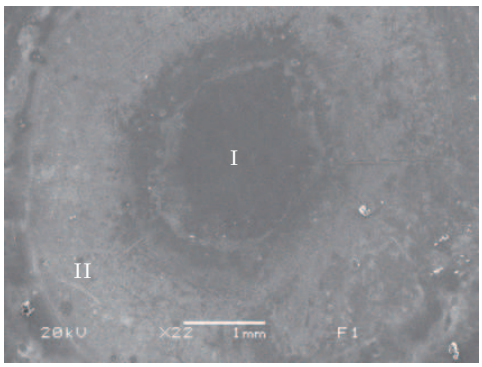


Fig. 8. Whole image of surface feature of aging sample.

Figure 9 shows the important details of microscopic views of the 100HN sample aged for 3 h and the broken-down sample (life time: 6 h and 10 min) under BCSIV respectively.

Figure 9(a) shows that significant damage occurs after being aged for 3 h under BCSIV on the sample surface and three layers are formed in sections. The layers are specified as I, II, and III, respectively. The surface layers, i.e., layers I and III, are low density layers resulting from the fast degradation through both electrical and chemical erosions. Layer II is a high density layer like the unaged sample. Figure 9(b) shows the structure damage around breakdown point after failure under BCSIV. The whole microscopic view of the breakdown point is shown in the micrograph through the first picture from the top in Fig. 9(b). The mesh structure and voids can be observed on the surface micrograph around the breakdown point obviously. The third picture from the top shows the non-breakdown part (part 1) and the breakdown part (part 2). Obviously, the voids also exist in the third layers of the section as shown in Fig. 9(b). The voids in layers are mainly caused by the degradation of insulation. When the voltage across these voids exceeds the PDIV, it leads to discharge and further degradation. The voids in which discharge occurs are enlarged after degradation through both chemical and physical erosion. The probability of forming voids is higher in low density layers due to the degradation caused by surface discharge. Therefore the sizes of voids in layer are larger than those in layer. Evidently, if the voids are subjected continuously to a level of voltage above the PDIV, insulation degradation caused by discharge will occur, and failure will be the eventual consequence.

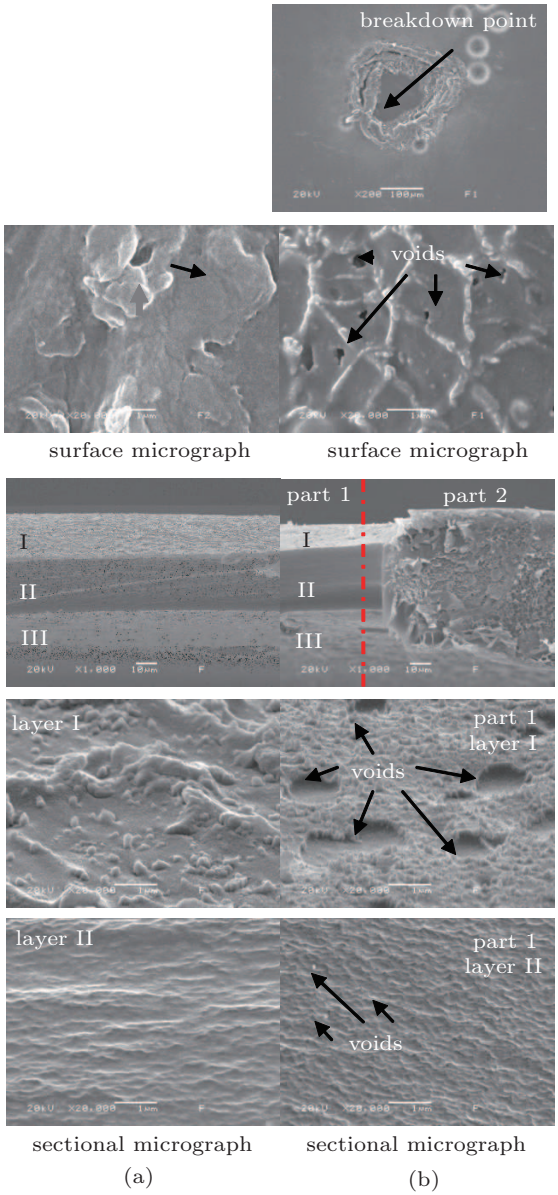


Fig. 9. (color online) Effects of aging time on SEM micrographs in 100HN samples. (a) Aged for 3 hours; (b) breakdown sample.

3.5. Analysis of space charge distribution

Space charge distributions within the aged specimens with a thickness of 125 μm for different aging times are shown in Fig. 10. As shown in Fig. 10, hetero-charges are trapped in the vicinities of both electrodes. The hetero-charge can

increase the electric fields near the electrodes, which is conducible to the charge injection. The quantity of hetero-charges increases continuously with the aging time increasing, which means that the trap density increases and the trapping position gradually moves into the bulk.

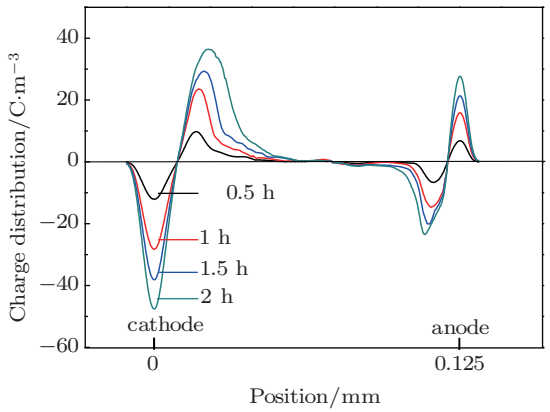


Fig. 10. (color online) Space charge distributions of polyimide film aged for various aging times.

4. Discussion

The essences of polymer degradation are the fracture of polymer chains. Usually, chemical degradation and physical degradation are caused together by discharge. There are some main processes generated by discharge as listed below.[9,10]

(i) High-energy electrons and ultraviolet rays, produced by discharge, attack the polymer chain together.

(ii) Discharge generates local high temperatures which would melt the local zone of the polymer dielectric.

(iii) •H and •O with high chemical activity would change the chemical structure and physical property through the chemical reaction with the polymer dielectric.

If surface discharge occurs, the mentioned effects concentrate on the surface layer of PI film together and cut off the polymer chains of PI molecule. The micro-structure and micro-morphology are changed because the organics are melted, carbonized, and volatilized. The insulation property of PI film is reduced and the film fails finally. Figure 11 shows the degradation process of PI during discharge.

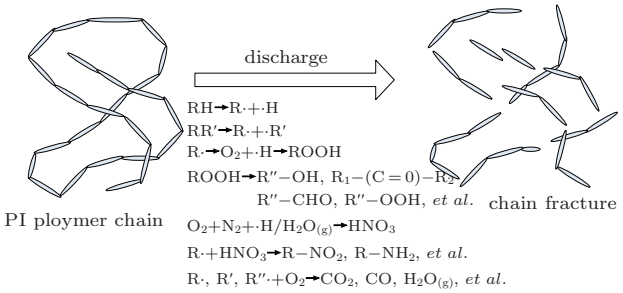


Fig. 11. Degradation process of PI molecule caused by discharge.

The synergistic effects of high-energy electrons, ultraviolet rays, and local high temperatures cut off the polymer chains of PI polymer. Consequently, the productive radical groups (R and R′) react with oxygen to form ROOH and R′OOH. According to the analysis of FTIR, the ether linkage (C–O–C) and imide ring (C–N–C) of the backbone of the PI polymer chain are destroyed at first, and the degree of polymerization of PI molecules is reduced. The intermediates are converted into the micro-molecule product including carboxylic acid, ketone, aldehydes, etc. Meanwhile, the C=O bond and C–H bond in the PI molecule may be oxidized and also form carboxylic acid, ketone, and aldehydes. Nitric acid will be generated through the effects of discharge. The nitric acid reacts with the intermediates to generate nitro-compounds and amino-compounds. All these intermediates, the mentioned micromolecule substance and active radical would be changed into gaseous phase including $H_2O_{(g)}$, CO, CO_2, etc.[27–29]

Meanwhile, charges are injected into the PI polymer bulk when PI film is aged. The injected charges (electron and hole) with high energy can release remnant energy during the processes of tapping and recombination. The remnant energy may be transferred through radiation and/or non-radiation to other electrons and make them hot electrons.[30] The hot electrons impact the PI macromolecule and makes it a free radical, which will result in the PI polymer degradation through the free radical chain reaction, generating lower molecule products and forming a partial low density region. It can increase polymer inhomogeneity and trap density.[31] The whole process can be illustrated as shown in Fig. 12.

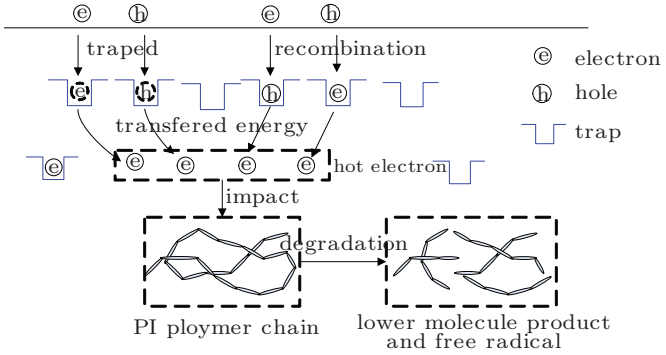


Fig. 12. Effects of space charge on degradation process of PI.

The trap density increases with aging time increasing. It implies that the probability of electron being trapped increases, which is conducible to the generation of more hot electrons. It will accelerate the impact of space charge on the degradation process of the PI polymer.

As analyzed above, the long PI polymer chains would be broken due to the effect of discharge, and many new short chains, functional groups or materials are generated with aging time increasing, which would affect the dielectric constant and dielectric loss. As indicated by the FTIR spectra in Fig. 4,

after the PI samples are aged for 1 h, the structures and morphologies of their chemical bonds are changed. The degree of cross linking decreases and the force among the polymer molecules is reduced, resulting in relaxation among the PI polymer chains and among the dipolar groups. As a result, the dielectric constant value increases more obviously, and the dielectric loss value decreases more clearly. After the aging time of PI samples increases from 2 h to 5 h, the backbones (like ether linkage (C–O–C) and imide ring (C–N–C) of backbone of PI polymer chain) and pendant groups (like C–H bond, C=O bond, etc.) of PI polymer molecules were cut off, more and more chemical groups (like carboxylic acid, ketone, aldehydes, etc.) are generated with aging time increasing, as depicted by FITR spectra and degradation processes in Figs. 4 and 11. It causes more dipolar groups with smaller molecular weight to easily produce orientation polarization with the applied electric field. The degree of polarization of the dipolar groups increases, and the friction interaction between the dipolar groups is weakened. Therefore, the dielectric constant value increases with aging time increasing, and the dielectric loss value decreases. The PI samples are damaged seriously after they have been aged for 6 h, and some gaseous phase products are separated out at this point. The number of dipolar groups in the aged solid PI sample may decrease. But the polarizable units of the samples aged for 6 h can orient more difficultly than those of the samples aged for 5 h. So, the dielectric constant ε decreases but the dielectric loss tan δ increases.

Fig. 13. (color online) Damage process of dielectric caused by discharge (a) discharge initiation; (b) discharge channel; (c) breakdown.

As shown in Fig. 9, we note that the surface microstructure and micro-morphology of PI film are damaged first, and then the damaged paths gradually extend to the interior with continuous discharge aging. The whole damage process of dielectric can be seen in Fig. 13. Discharge erodes the surface layer of PI film. The organics take the place of chemical degradation and physical degradation. Some of the degraded organics change into the gases and volatilize, the other residues remain on the surface of PI film. The roughness and surface conductivity will be changed because of the residues.[21,32] With the increase of aging time, the surface layer of PI film is damaged more seriously. The eroded volume of dielectric increases and the discharge paths begin to develop into the PI film for forming electrical trees. Therefore, it can be seen in Fig. 9 that the micro-structure and micro-morphology are different between the surface layer of the PI sample and the inner layer of the PI sample. When the discharge channels extend to the opposite electrode, the dielectric film is broken down. The microscopic views of damage processes of PI film caused by discharge are shown in Fig. 14. The discharge channels of PI film aged for 3 h can be seen clearly in Fig. 14(b).

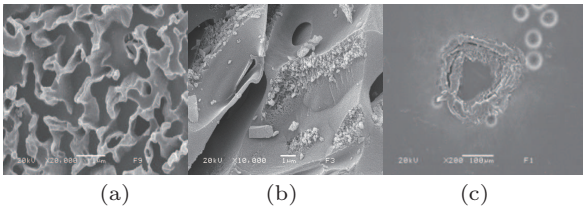


Fig. 14. Microscopic views of damage process of PI film caused by discharge. (a) Discharge initiation; (b) discharge channel; (c) breakdown.

5. Conclusions

In this work, structural and morphological changes of PI film aged under BCSIV above PDIV are investigated by SEM and FTIR. The dielectric properties of PI samples are analyzed, and the microscopic degradation mechanism of PI film is investigated. Some interesting conclusions can be obtained as follows.

i) The FTIR spectra show that the intensities of some reflectance peaks decrease due to the fact that the structures and morphologies of chemical bonds have been changed by discharges erosion. Meanwhile, new reflectance peaks are observed in the FTIR spectra of the aged sample. It suggests that ether linkage (C–O–C bonds), C–N–C bonds in imide ring, and other bonds in aromatic rings are broken.

ii) The degree of cross linking and dipolar groups is changed by discharge, which can change the dielectric properties of aged samples. The dielectric constant ε for aged PI samples is bigger than for unaged samples and there is a big increase for the sample aged for 1 h. The ε increases gradually with aging time increasing, except for the samples aged for 6 h. Because more dipolar groups are generated for the samples with aging time increasing from 1 h to 5 h, the dipolar groups can orient following the polarity alteration of applied electric field. Therefore, the dielectric loss tan δ decreases gradually and tan δ for the sample aged for 1 h decreases more obviously. For the sample aged for 6 h, tan δ increases on the contrary.

iii) Surface discharge damages the PI film, and the microstructure and micro-morphology of surface layer are changed. The damage to PI film structure concentrates on the surface of the sample under BCSIV in the presence of surface discharge. Therefore the degradation of structure in PI film is initiated from the surface and then gradually extends to the interior with continuous aging.

References

[1] Gao Q, Asher G M, Sumner M and Makys P 2007 *IEEE Trans. Ind. Appl.* **43** 1001

[2] Ahmed T, Nishida K and Nakaoka M 2006 *IEEE Trans. Ind. Appl.* **42** 934
[3] Kaufhold M, Aninger H, Berth M, Speck J and Eberhardt M 2000 *IEEE Trans. Ind. Electron.* **47** 396
[4] Melfi M, Sung A M J, Bell S and Skibinski G L 1998 *IEEE Trans. Ind. Appl.* **34** 766
[5] Yin W J 1997 *IEEE Trans. Electr. Insul. Mag.* **13** 18
[6] Hayakawa N and Okubo H 2005 *IEEE Electr. Insul. Mag.* **21** 5
[7] Hudon C, Amyot N, Lebey T, Castelan P and Kandev N 2000 *IEEE Trans. Dielectr. Electr. Insul.* **7** 783
[8] Coletti G, Guastavino F and Torello E 2002 *Conference Record of the IEEE International Symposium on Electrical Insulation*, April 7–10, 2002, Boston, USA, p. 36
[9] Morshuis P H F 2005 *IEEE Trans. Dielectr. Electr. Insul.* **12** 905
[10] Liu F D, Yang B T, Tu D M and Liu Y N 1992 *Acta Phys. Sin.* **41** 333 (in Chinese)
[11] Jia Z D Hao Y P and Xie H K 2006 *IEEE Trans. Dielectr. Electr. Insul.* **13** 415
[12] Tanaka T, Ohki Y, Ochi M, Harada M and Imai T 2008 *IEEE Trans. Dielectr. Electr. Insul.* **15** 81
[13] Liu Y Q, An Z L, Cang J, Zhang Y W and Zheng F H 2012 *Acta Phys. Sin.* **61** 158201 (in Chinese)
[14] Venkatesulu B and Thomas M J 2010 *IEEE Trans. Dielectr. Electr. Insul.* **17** 625
[15] Ramirez I, Jayaram S, Cherney E A, Gauthier M and Simon L 2009 *IEEE Trans. Dielectr. Electr. Insul.* **16** 52
[16] Overney R M, Güntherodt H J and Hild S 1994 *J. Appl. Phys.* **75** 1401
[17] Takala M, Sallinen T, Nevalainen P, Pelto J and Kannus K 2008 *IEEE International Symposium on Electrical Insulation*, June 9–12, 2008 Vancouver, Canada, p. 205
[18] Kozako M, Fuse N, Ohki Y, Okamoto T and Tanaka T 2004 *IEEE Trans. Dielectr. Electr. Insul.* **11** 833
[19] Fuse N, Ohki Y, Kozako M and Tanaka T 2008 *IEEE Trans. Dielectr. Electr. Insul.* **15** 161
[20] Yan J M, Liao R J, Yang L J, Li J and Liu B 2011 *Appl. Surf. Sci.* **257** 5863
[21] Liao R J, Yan J M, Yang L J, Zhu M Z and Sun C X 2011 *Proc. Chin. Soc. Electr. Eng.* **31** 129 (in Chinese)
[22] Zhang P H, Fan Y, Wang F C, Xie H, Li G and Lei Q Q 2005 *Chin. Phys. Lett.* **22** 1253
[23] Zheng F H, Zhang Y W, Wu C S, Li J X and Xia Z F 2003 *Acta Phys. Sin.* **52** 1137 (in Chinese)
[24] Chen T X, Yao S D, Wang K, Wang H, Ding Z B and Chen D 2009 *Chin. Phys. Lett.* **26** 26101
[25] Zhu Y, Otsubo M and Honda C 2006 *Polym. Test.* **25** 313
[26] Buncick M C and Denton D D 1990 *IEEE 4th Technical Digest of Solid-State Sensor and Actuator Workshop*, June 4–7, 1990, Hilton Head Island, USA, p. 102
[27] Dinetz S F, Bird E J, Wagner R L and Fountain A W 2002 *J. Anal. Appl. Pyrolysis* **63** 241
[28] Lua A C and Su J C 2006 *Polym. Degradation Stab.* **91** 144
[29] Pramoda K P, Chung T S, Liu S L, Oikawa H and Yamaguchi A 2000 *Polym. Degradation Stab.* **67** 365
[30] Kao K C 1984 *J. Appl. Phys.* **55** 752
[31] Liufu D, Wang X S, Tu D M and Kao K C 1998 *J. Appl. Phys.* **83** 2209
[32] Hudon C, Bartnikas R and Wertheimer M R 1993 *IEEE Trans. Electr. Insul.* **28** 1